ELEMENTARY PARTICLES AND FIELDS
Experiment

VEPP-2000 Project: Collider, Detectors, and Physics Program

S. I. Serednyakov

Budker Institute of Nuclear Physics, Siberian Division, Russian Academy of Sciences,
pr. Akademika Lavrent'eva 11, Novosibirsk, 630090 Russia
Novosibirsk State University, ul. Pirogova 2, Novosibirsk, 630090 Russia
Received March 26, 2003; in final form, August 12, 2003

Abstract—The new VEPP-2000 e^+e^- collider of maximum energy 2000 MeV, which is under construction at the Budker Institute of Nuclear Physics (Siberian Division, Russian Academy of Sciences, Novosibirsk), is briefly described. Experiments at VEPP-2000 will be performed with two upgraded detectors, CMD-2M and SND. A precise measurement of the total cross section for the process $e^+e^- \to$ hadrons and of the partial cross sections for its exclusive hadronic channels is the main point of the physics program for this machine. These measurements will be aimed at testing QCD and the VMD and CVC models, as well as at refining the hadron contribution to fundamental constants such as the muon anomalous magnetic moment $a_\mu = \dfrac{g-2}{2}$ and the fine-structure constant $\alpha_{\rm em}(M_Z^2)$. Measurements of the nucleon form factors in the reactions $e^+e^- \to p\bar{p}, n\bar{n}$ at their threshold will also be of great importance. © 2004 MAIK "Nauka/Interperiodica".

1. VEPP-2000 COLLIDER

The project of VEPP-2000 was proposed to extend the physics program of the VEPP-2M collider [1] toward higher energies up to 2.0 GeV in the c.m. frame. In the new accelerator complex, the VEPP-2M collider will be replaced by VEPP-2000. Figure 1 shows the layout of the VEPP-2000 accelerator complex. It should be noted that the injection part of the complex (linear accelerator, electron synchrotron, booster) will not undergo significant changes.

The main parameters of VEPP-2000 are the following [2, 3]:

(a) The operating energy (in the c.m. frame) will range between 0.4 and 2.0 GeV.

(b) The luminosity will be $L = 10^{31} \rm cm^{-2} s^{-1}$ and $L = 10^{32} \rm cm^{-2} s^{-1}$ at $2E = 1.0$ GeV and $2E = 2.0$ GeV, respectively.

(c) The perimeter will be 24.5 m.

(d) The current will be 200 mA ($E = 0.9$ GeV).

(e) The size of the beam along the orbit will be 3.4 cm ($E = 0.9$ GeV).

(f) The energy scatter will be 0.7 MeV ($E = 0.9$ GeV).

Although the VEPP-2000 luminosity is lower than the luminosities of e^+e^- factories, however, it is two to three orders of magnitude higher than that of colliders that operated earlier at energies of $2E > 1.4$ GeV, such as DCI (Orsay) and ADONE (Frascati). The expected integrated luminosity of

VEPP-2000 will be about 3 fb^{-1} over a 5-year period of experiments.

A feature peculiar to VEPP-2000 is an unusual focusing system that involves both traditional quadrupole lenses and a radically new element, superconducting solenoids creating a magnetic field of strength 8 T. As electrons traverse a solenoid, the plane of betatron oscillations is rotated through $90°$, whereby there occurs the mixing of the vertical and horizontal betatron oscillations, with the result that the beam cross section becomes circular. The current producing the maximum effect of the intersection of beams increases, which leads to an increase in the collider luminosity. This scheme of increasing the luminosity will be tested at VEPP-2000.

Presently, the collider elements are being manufactured and mounted in the experimental hall.

2. SND DETECTOR

Experiments with the spherical neutral detector (SND) [4] were carried out at the VEPP-2M e^+e^- collider of integrated luminosity about 30 pb^{-1} over the period from 1995 to 2000.

An electromagnetic calorimeter based on 1632 NaI(Tl) crystals is the main part of the SND detector; it is manufactured in the form of three spherical layers (Fig. 2). The total weight of the NaI(Tl) crystals is 3.6 t, and the solid angle of the calorimeter is about 90% of 4π. The energy resolution for photons is
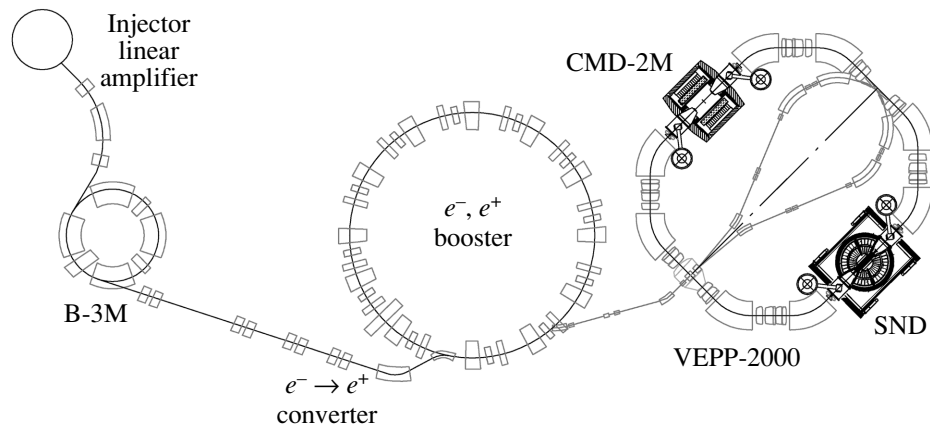
Fig. 1. Layout of the VEPP-2000 accelerator complex. The SND and CMD-2M detectors are shown in the right part of the figure along with the VEPP-2000 collider.
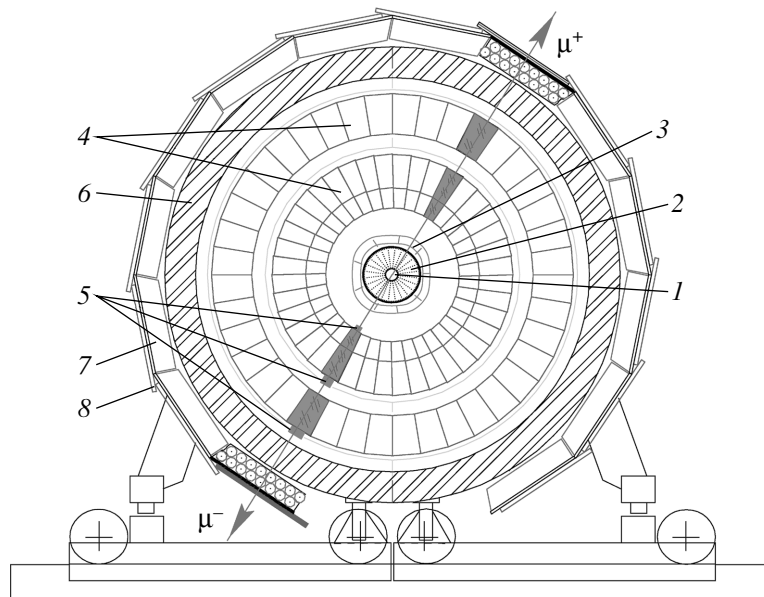

Fig. 2. SND detector view in the plane transverse to the beam direction: (*1*) vacuum chamber, (*2*) drift chambers, (*3*) aerogel Cherenkov counters, (*4*) NaI(Tl) counters, (*5*) phototriodes, (*6*) iron absorber, (*7*) streamer tubes, and (*8*) scintillation counters.

$\sigma_E/E = 4.2\%/\sqrt[4]{E(\text{GeV})}$ [5], and the angular resolution is about 1.5°. The photon-energy threshold is set at a level of 20 MeV. A system of two cylindrical drift chambers with a solid angle of 95% of 4π is used to measure the emission angle of charged particles. The measurement accuracy is 0.4° for the azimuthal angle and about 2° for the polar angle. A muon detector consisting of streamer tubes [6] is placed outside the calorimeter.

An upgrade of SND is presently being performed [7]. A new drift chamber is being manufactured to be used as a track detector. An aerogel Cherenkov counter (with the refractive index being $n = 1.13$) will be an additional element of SND. It will permit separating π^- and K mesons of momentum up to 900 MeV/c. In the new SND detector, electronics and the system of data readout and data processing will also be upgraded.

3. CMD-2M DETECTOR

Figure 3 shows layout of the CMD-2M detector [8], which is a superconducting solenoid $0.15X_0$ thick generating a magnetic field of strength 1.5 T; it encloses a drift chamber that ensures measurement of the emission angles and momenta of charged particles. The angular accuracy is about 5 mrad; the momentum resolution is about 3% for a momentum
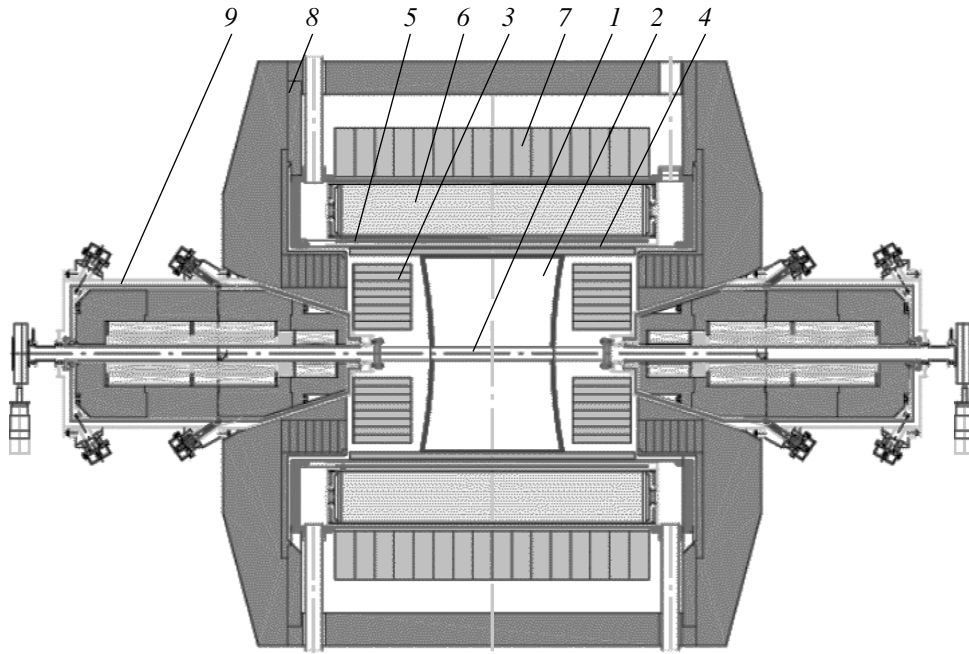
Fig. 3. CMD-2M detector view along the beam direction: (*1*) vacuum chamber, (*2*) drift chambers, (*3*) BGO calorimeter, (*4*) *Z* chamber, (*5*) superconducting solenoid, (*6*) LXe calorimeter, (*7*) CsI calorimeter, (*8*) magnet yoke, and (*9*) superconducting focusing solenoids.

of 1 GeV; the mean number of wires along a track is 19.

The CMD-2M calorimeter is combined. Its end-cap part is formed by BGO crystals with readout based on silicon photodiodes. The barrel part of the calorimeter incorporates liquid krypton ($8X_0$) and CsI(Tl) crystals ($5X_0$) along the particle path. The CMD-2M calorimeter has a very high solid-angle granularity, this permitting an efficient detection of events featuring a high multiplicity or closely outgoing particles. The energy resolution of the calorimeter for 0.1- to 1-GeV photons is expected to be in the range 3–6%. The angular resolution ranges from 0.3° (in the barrel part) to 1° (in the endcap part).

In order to improve the separation of π^- and K mesons and to suppress the cosmic-ray background, a time-of-flight system based on plane scintillation counters is placed outside the calorimeter.

4. PHYSICS PROGRAM

4.1. Total Cross Section for e^+e^- Annihilation into Hadrons

The ratio $R = \dfrac{\sigma(e^+e^- \to \text{hadrons})}{\sigma(e^+e^- \to \mu^+\mu^-)}$ is a funda-mental constant within the quark model and QCD. To a first approximation, $R = 3\sum_q e_q^2$; for the first three quarks u, d, and s, we then have $R \simeq 2$. The calculated value of R with allowance for QCD corrections

is in agreement with experimental data in the energy region $2E > 1.5$ GeV. The VEPP-2000 range $2E = 1.4$–2.0 GeV is the resonance or transition energy region, where the cross sections for the main processes making a dominant contribution to R change abruptly with energy. The experimental uncertainties in these cross sections are still large and result in an uncertainty of $\Delta R/R \simeq 10\%$. The challenge of VEPP-2000 is to reduce this uncertainty to 2–3%.

4.2. Contribution of R to the Muon Anomalous Magnetic Moment $a_\mu = \dfrac{g-2}{2}$

The muon anomalous magnetic moment is one of the fundamental constants in elementary-particle physics. It is about 10^{-3} of the total magnetic moment of the muon; this small value was measured to a precision of 0.7 ppm[1]) in the E821 experiment (BNL) [9]. The accuracy of the calculated muon anomalous magnetic moment is nearly identical to the experimental one: 0.9 ppm [10]. However, there are some problems in the calculation. The point is that the leading contribution to the calculated accuracy comes from the hadronic vacuum polarization, which cannot be obtained from basic QCD concepts at present. To calculate the hadronic vacuum polarization, use is made of experimental data on the total cross section
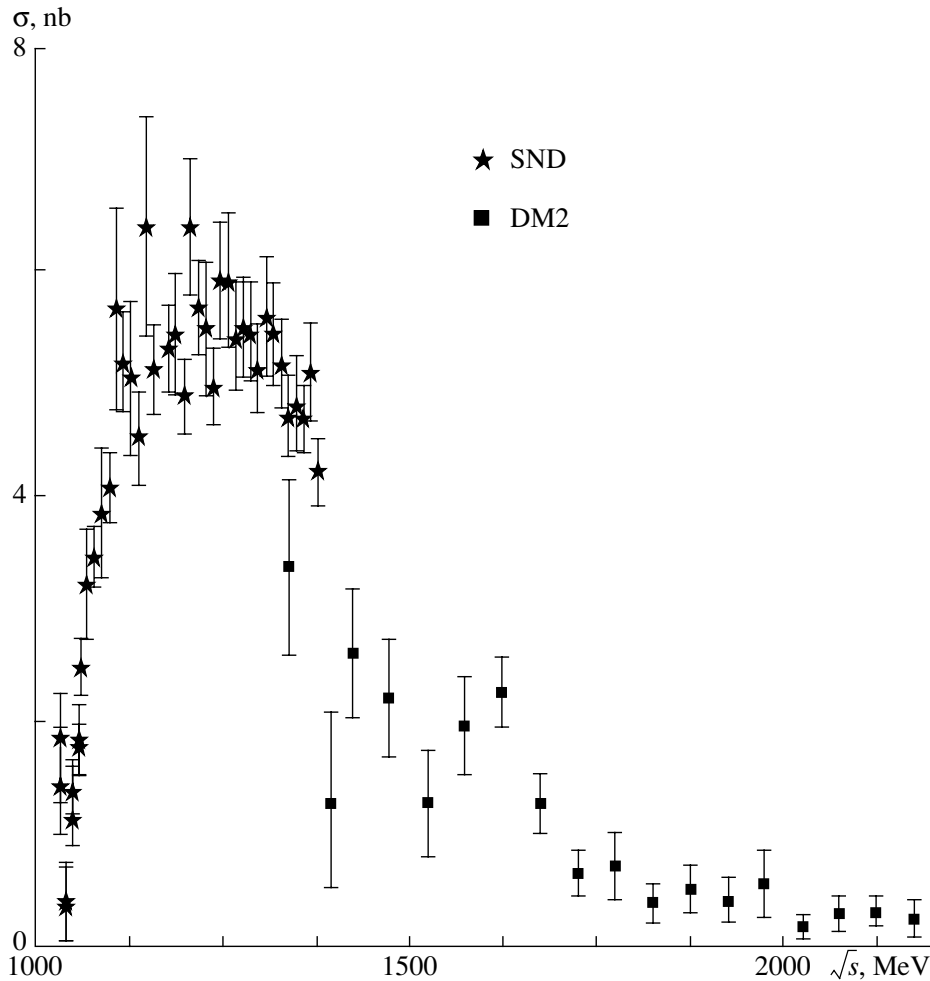
---

[1])1 ppm $= 10^{-6}$.

Fig. 4. Experimental cross sections for the process $e^+e^- \to \pi^+\pi^-\pi^0$.

for the process $e^+e^- \to$ hadrons. Lower energies (the ρ-meson region) make the greatest contribution to R, which is actually measured at VEPP-2M and VEPP-2000.

The most accurate measurements of R were performed by the CMD-2 Collaboration (Novosibirsk) [11]. The muon anomalous magnetic moment calculated with the data of these measurements is less than the result of the E821 experiment by three standard deviations (2.9 ppm). The respective value from τ-lepton decays is also less than the E821 result, but, in this case, the difference is less (1.5σ). New measurements of R at VEPP-2000 are absolutely necessary, because a reliably established discrepancy between the experimental and the theoretical results for the muon anomalous magnetic moment would mean a breakdown of the Standard Model.

4.3. Contribution of R to the Fine-Structure Constant $\alpha_{em}(M_Z^2)$

As is well known, the fine-structure constant α_{em} grows slowly with increasing energy, and its value is $1/129$ at the Z_0-boson peak (instead of the usual value, which is equal to $1/137$ in the zero-energy limit). However, the accuracy of $\alpha_{em}(0)$ is 4×10^{-8} [12], but the accuracy of $\alpha_{em}(M_Z^2)$ is substantially poorer ($\sim 10^{-3}$).

In order to test the electroweak model precisely, it is of great importance to improve the accuracy of $\alpha_{em}(M_Z^2)$. For instance, verification of the relation

$$\sin^2\theta_W(1 - \sin^2\theta_W) = \frac{\pi\alpha_{em}(M_Z^2)}{\sqrt{2}G_F M_Z^2}$$

is hindered by the accuracy of $\alpha_{em}(M_Z^2)$ (the dependence on M_t and M_H is not taken into account). The uncertainties in the other quantities appearing in this relation are considerably smaller:

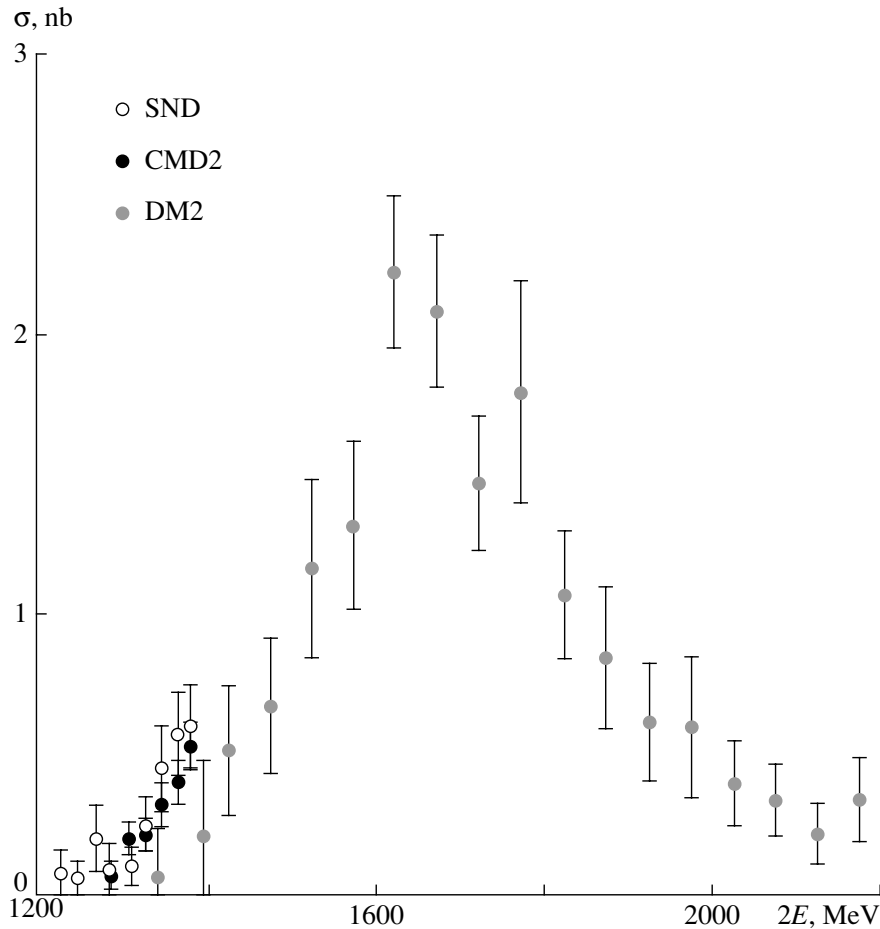$$\delta G_F \sim 10^{-5}; \qquad \delta M_Z \sim 10^{-4}.$$

Fig. 5. Experimental cross sections for the process $e^+e^- \to \omega\pi^+\pi^-$.

As in the case of the muon anomalous magnetic moment, the experimental cross section for the process $e^+e^- \to$ hadrons is employed in the QED calculation of the constant $\alpha_{\mathrm{em}}(M_Z^2)$. However, higher energies make the most significant contribution to the hadronic vacuum polarization here. According to the 1999 data, however, the energy region $2E < 2$ GeV makes a contribution of above 30% to the uncertainty in $\alpha_{\mathrm{em}}(M_Z^2)$. It follows that, if an improved precision at higher energies is achieved, for example, with VEPP-4M, new, more precise measurements of R at VEPP-2000 (that is, with an accuracy higher than 1% in the ρ-meson region and higher than 2 to 3% between 1 and 2 GeV) will make it possible to improve the accuracy of testing electroweak theory in the future considerably.

4.4. Individual Processes of e^+e^- Annihilation into Hadrons and Spectroscopy of Excited Vector Mesons

The value of R is determined by the sum of the cross sections for all hadronic processes, for example,

$$e^+e^- \to 2\pi, 3\pi, 4\pi, 5\pi, K\bar{K}, K\bar{K}\pi, N\bar{N}, \ldots.$$

These processes are dominant at VEPP-2000. In the region $2E < 1$ GeV, the processes $e^+e^- \to 2\pi, 3\pi$ have the largest cross section; at higher energies, these cross sections decrease, so that the process $e^+e^- \to 4\pi$ appears to be dominant. For each individual process, the cross section is described rather well by the vector-meson-dominance (VMD) model with some corrections, including the energy dependence of the resonance width. In addition to the well-known resonances $\rho(770)$, $\omega(782)$, and $\phi(1020)$, the existence of heavier and wider resonances (excited quarkonia) has been established experimentally [12]:

$\rho(1450)$: $M = 1465 \pm 25$; $\Gamma = 310 \pm 60$; 4π;
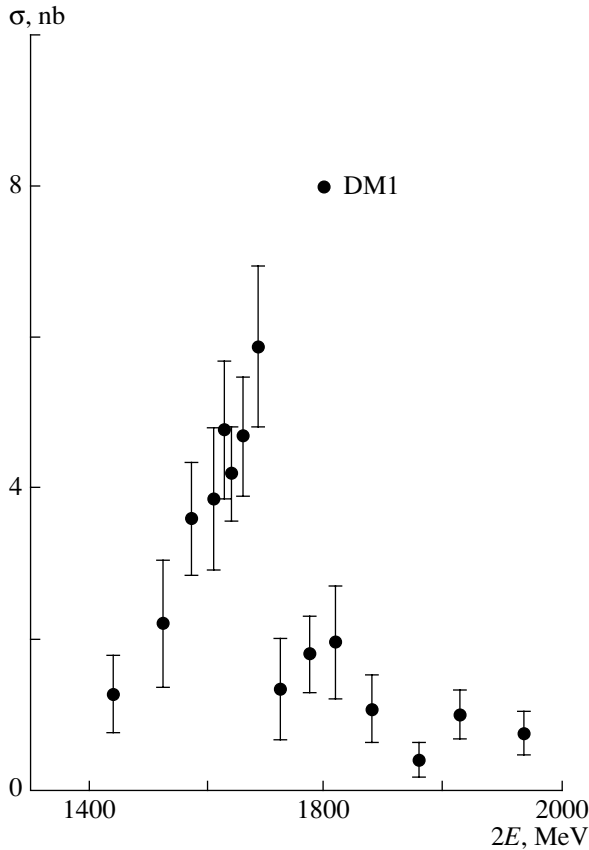
$\rho(1700)$: $M = 1700 \pm 20$; $\Gamma = 240 \pm 60$; 4π;

Fig. 6. Experimental cross sections for the process $e^+e^- \to K_S K^+ \pi^-$.

$\rho(2150)$: $M = 2149 \pm 17$; $\Gamma = 363 \pm 50$; K^+K^-;

$\quad \omega(1420)$: $M = 1419 \pm 31$; $\Gamma = 174 \pm 60$; 3π;

$\omega(1650)$: $M = 1649 \pm 24$; $\Gamma = 220 \pm 35$; $\omega\pi^+\pi^-$;

$\quad \phi(1680)$: $M = 1680 \pm 20$; $\Gamma = 150 \pm 50$; K^*K.

(Here M and Γ are given in MeV.)

The parameters of excited resonances, especially their decay modes, have not yet been determined properly (large systematic uncertainties of about 20%, very large energy step between the measurements, poor statistical accuracy). For some processes, Figs. 4–6 display experimental data obtained over 30 years in the experiments performed at the VEPP-2, VEPP-2M, ACO, ADONE, and DCI colliders.

The experimental accuracy achieved in studying these processes is far from required values of 3 to 5%. This is due to a low integrated luminosity of about 5 pb^{-1} in the energy range $1.4 < 2E < 2$ GeV and insufficient quality of the detectors used previously. The integrated luminosity expected at VEPP-2000 is about 3 fb^{-1}, which is three orders of magnitude
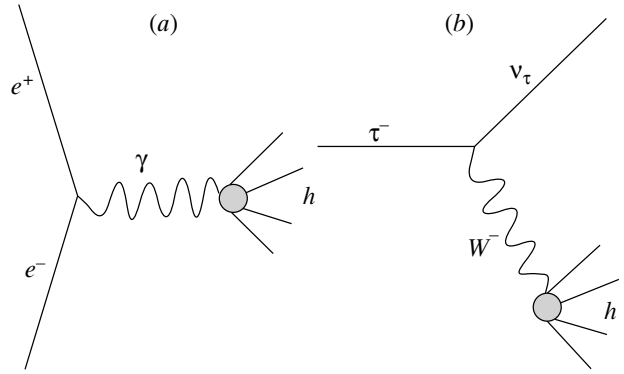

Fig. 7. Diagrams illustrating the CVC hypothesis: (*a*) diagram representing the process $e^+e^- \to$ hadrons and (*b*) diagram representing τ decay.

higher than that which is available at present. Additionally, the VEPP-2000 detectors (SND, CMD-2M) are modern detectors that cover a large solid angle and a high potential for identifying particles; therefore, a considerable improvement of accuracy is quite feasible.

4.5. Testing of the Hypothesis of the Conservation of the Vector Current

The hypothesis of the conservation of the vector current (CVC) relates the τ-leptonic-decay mass spectra of $J^{\mathrm{PG}} = 1^{-+}$ hadrons to the isovector part of the cross section for e^+e^- annihilation into hadrons as a function of energy (Fig. 7). For example, the spectrum of hadron masses M_h in the decay $\tau^+ \to \omega\pi^+\nu$ is related to the cross section $\sigma^{I=1}_{e^+e^-}$ for the process $e^+e^- \to \omega\pi^0$ by the equation

$$\frac{dM_h}{dq^2} = \frac{G_{\mathrm{F}}^2 \cos^2\theta_{\mathrm{c}}(1 + \delta_{\mathrm{EW}})}{32\pi^2\alpha^2 m_\tau^3}$$
$$\times (m_\tau^2 - q^2)(m_\tau^2 + 2q^2)v_1(q^2),$$
$$v_1(q^2) = \frac{q^2 \sigma^{I=1}_{e^+e^-}(q^2)}{4\pi\alpha^2}.$$

Presently, this expression is being experimentally verified for many isovector processes of e^+e^- annihilation and this serves as a test of the electroweak model. On the other hand, there appears the possibility of cross-checking data on e^+e^- annihilation and τ lepton under the assumption that the CVC hypothesis is valid.

In Fig. 8, the cross section measured with the SND detector at VEPP-2M [13] for the process $e^+e^- \to \omega\pi^0$ is contrasted against the CVC prediction based on τ-lepton decays in the CLEO experiment. This is one of the best examples of testing the CVC hypothesis. Another example has already
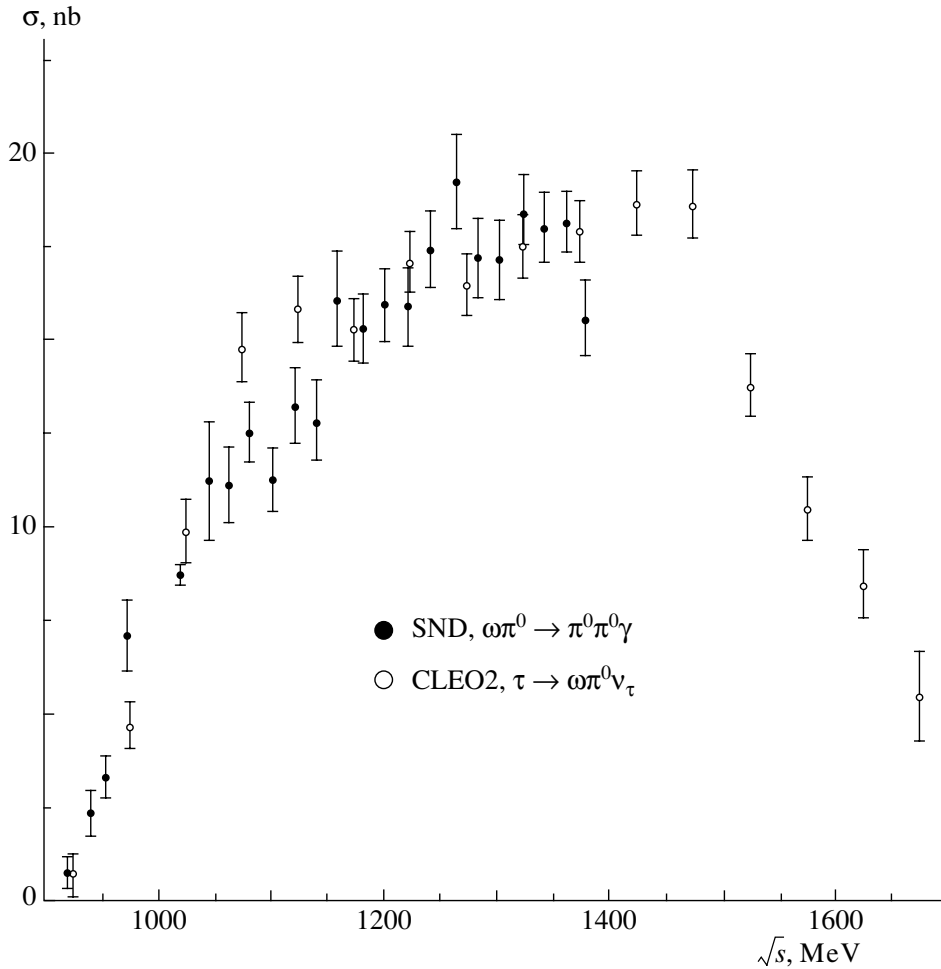
Fig. 8. Comparison of the cross section for the process $e^+e^- \to \omega\pi^0$ (SND) and the CVC prediction on the basis of τ decays (CLEO).

been given above in discussing the muon anomalous magnetic moment. In the latter case, the process $e^+e^- \to \pi^+\pi^-$ makes the main contribution to the muon anomalous magnetic moment, with result that the data on e^+e^- annihilation appear to be 1.5% lower than those on the τ lepton.

In summary, we can say that the next step in testing the CVC hypothesis for the main isovector processes to a precision of about 1% can be made at VEPP-2000.

4.6. Threshold Production of Nucleon Pairs

At VEPP-2000, the production of nucleon pairs in the processes $e^+e^- \to p\bar{p}, n\bar{n}$ becomes possible, which will permit extracting data on the electromagnetic form factors for the proton and the neutron in the timelike region of momentum transfer at the nucleon-production threshold. It should be noted that the timelike form factors for meson pairs ($\pi^+\pi^-$, $K\bar{K}$)

were measured adequately, and strong resonances [such as $\rho(770)$ and $\phi(1020)$] were observed.

The situation is somewhat different for nucleon pairs. In the threshold region $2E < 2$ GeV, available data are very scanty, and there are no data at all on nucleons of kinetic energy in the region $T < 10$ MeV. The neutron yield was measured in a single experiment (FENICE, ADONE) [14]. Figures 9 and 10 illustrate the available experimental results for the form factors.

The DM2 and FENICE experiments at $\sqrt{s} \simeq 2$ GeV yielded $\sigma_{p\bar{p}} \simeq \sigma_{n\bar{n}} \simeq 1$ nb and $|G^p| \simeq |G^n| \simeq 0.4$.

For the cross-section ratio $r = \dfrac{\sigma(e^+e^- \to n\bar{n})}{\sigma(e^+e^- \to p\bar{p})}$, various models of the nucleon form factors (perturbative QCD, extended VMD model, Skyrme model) give a wide range of values: $r = 1/4-100$.

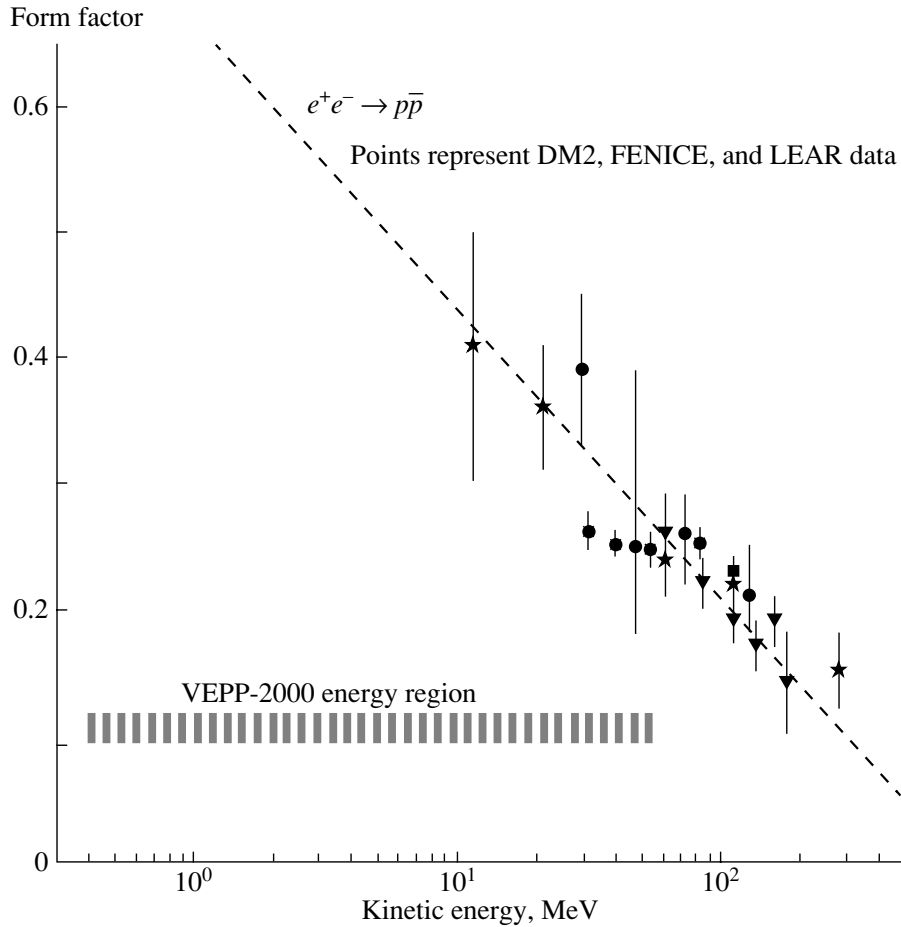The following problems will be studied at VEPP-2000. Is the neutron form factor indeed greater than

Fig. 9. Experimental data on the proton form factor.

the proton form factor? Will it be confirmed that the form factor grows as the energy decreases down to the very threshold? Will it be possible to measure the electric and magnetic form factors separately? Are there $N\bar{N}$ bound states in the vicinity of the threshold?

In particular, the DM2 data on the process $e^+e^- \rightarrow 3\pi^+3\pi^-$ (Fig. 11) [15] favor the existence of $N\bar{N}$ bound states. Specifically, these data suggest a resonance structure in the cross section precisely at the nucleon-production threshold. We can add that, if an $N\bar{N}$ bound state is an above-threshold one, it can be observed distinctly in the processes $e^+e^- \rightarrow p\bar{p}, n\bar{n}$ in the form of an irregularity in the threshold cross section.

At an integrated luminosity of $\Delta L \sim 1$ fb^{-1} and a detection efficiency of $\epsilon \sim 0.1$, the number of events involving nucleon−antinucleon pairs can be estimated at $N_{p\bar{p}} \sim N_{n\bar{n}} \sim 10^4$ on the basis of the threshold cross section of $\sigma_{p\bar{p}} \simeq \sigma_{n\bar{n}} \simeq 10^{-34}$ cm^2 at $T \sim 1$ MeV (the energy scatter being $\sigma E \simeq 0.7$ MeV). This is two orders of magnitude greater than the

statistics of such events in previous experiments. This is the reason why one can hope that experiments at VEPP-2000 will provide answers to many of the questions formulated above.

The cross sections for proton-pair production at the threshold has the characteristic form of a step at $2E = 2M_p$, this enabling calibration of the collider energy scale. An estimation shows that, within a measurement period of about one day, the energy can be calibrated to a precision of $\Delta E \simeq 0.1$ MeV. This value is an order of magnitude less than the energy scatter of $\sigma E \simeq 0.7$ MeV.

A very narrow ($\Gamma \sim 10^{-2}$ eV) $p\bar{p}$ Coulomb-like bound state of binding energy about -12.5 keV can be formed at the threshold for proton-pair production. Unfortunately, the energy scatter leads to a decrease in the cross section for the production of this resonance by many orders of magnitude to a level of 1 % of the cross section for the process $e^+e^- \rightarrow$ hadrons. At a high statistical accuracy, there is, however, a chance to observe this phenomenon if the cross section for the process $e^+e^- \rightarrow$ hadrons behaves smoothly in the vicinity of the threshold for proton-pair production.
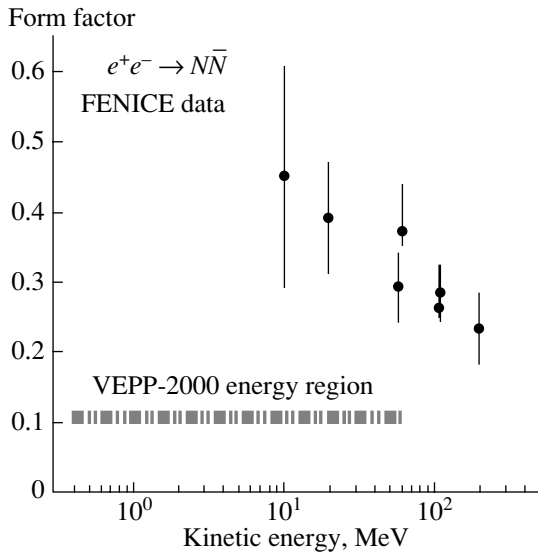
Fig. 10. Experimental data on the neutron form factor.

4.7. Hadron Production in Processes of "Radiative Return to a Resonance" (Fig. 12)

The production of hadrons of effective mass in the region $M < \sqrt{s}$ is also possible in processes involving the emission of a photon of energy $\omega = \dfrac{s - M^2}{2\sqrt{s}}$ [16]. Sometimes, such processes are referred to as those of the initial-state-radiation (ISR) type. Although the cross sections for ISR processes is considerably smaller than those for direct hadron production, these processes have a number of special features that make their experimental study worthwhile. First, the integrated luminosity of colliders usually grows fast with increasing energy; therefore, the number of ρ, ω, and ϕ mesons produced at B factories, for example, is quite commensurate with the number of these particles produced directly at VEPP-2M. Second, hadrons from ISR processes are tagged, since they are accompanied by a recoil photon, this simplifying the analysis of respective events. Third, the entire mass spectrum of hadrons is accessible, so that normalization to the calibration process $e^+e^- \to \mu^+\mu^-\gamma$ is possible.

A simple ISR process such as $e^+e^- \to \omega\gamma \to \pi^0\pi^0\gamma$ was clearly seen even at VEPP-2M with SND (Fig. 13). At an integrated luminosity of $\Delta L \sim 3\,\mathrm{fb}^{-1}$, about 10^7 ρ mesons and 10^6 ω mesons are expected at VEPP-2000; this will make it possible to perform independent measurements of hadron cross sections and the parameters of vector mesons.

4.8. Two-Photon Physics

The production of C-even mesons (C^+) at an e^+e^- collider is possible in processes of two types:

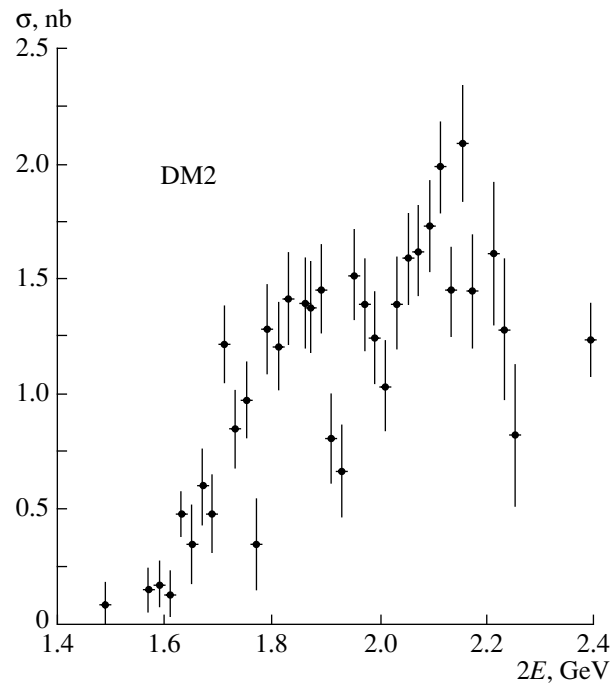**Fig. 11.** Cross section for the process $e^+e^- \to 3\pi^+3\pi^-$ in the vicinity of the hadron-production threshold according to data from [15].

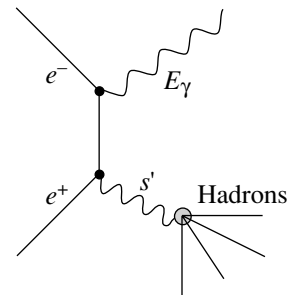**Fig. 12.** Diagram representing hadron production in a process of radiative reversion to a resonance.

$e^+e^- \to e^+e^- + C^+$ and $e^+e^- \to C^+$. Processes of the first type have long since been studied in e^+e^- experiments. This made it possible to measure the widths $\Gamma(C^+ \to 2\gamma)$ for many C-even mesons and the cross sections for the processes $\gamma\gamma \to$ hadrons.

It is of interest to measure the two-photon widths of the $f_0(980)$ and $a_0(980)$ mesons at VEPP-2000. These scalar mesons have an anomalously small two-photon width of about 0.3 keV in relation to their nearest pseudoscalar neighbor $\eta'(960)$ (its width is 4.4 keV). Therefore, a new and more precise measurement of $\Gamma_{2\gamma}$ at VEPP-2000 will be useful. It will also be possible to measure anew the cross section for the processes $\gamma\gamma \to \pi\pi, \eta\pi, \ldots$ in the region $\sqrt{s} < 1$ GeV, where available experimental data are scanty.
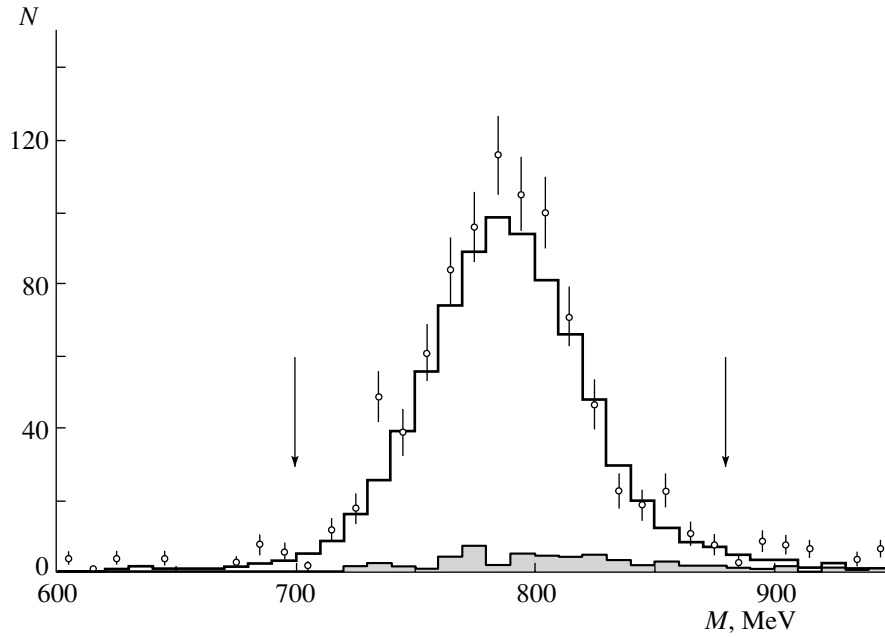
Fig. 13. Mass spectrum of ω mesons in the process $e^+e^- \rightarrow \omega\gamma$: (points) SND experimental results and (histogram) results of a simulation of the process. The arrows show the cuts used in calculating the total cross section. The shaded histogram corresponds to the background contribution.

The statistics of events produced in these processes will be about 10^3–10^4.

Previously, C-even processes of the second type, $e^+e^- \rightarrow C^+$, were studied only at VEPP-2M [17], where upper limits on the electron widths of the $f_2(1270)$ and $a_2(1320)$ mesons were established at a level close to the results of respective calculations. We hope to observe the direct production of these mesons in the process $e^+e^- \rightarrow f_2(1270), a_2(1320)$ at VEPP-2000 with a high integrated luminosity.

4.9. Test of QED in Processes with a High Multiplicity in the Final State

There are many QED processes producing at large angles a great number of final-state particles ($\theta \sim 1$), for example,

$$e^+e^- \rightarrow \gamma\gamma\gamma\gamma, \quad e^+e^-e^+e^-, \quad e^+e^-\gamma\gamma, \ldots.$$

The cross sections for these processes range between 10^{-36} and 10^{-34} cm^2 (within the solid angle of the detector); therefore, the number of respective events amounts to hundreds or thousands even with allowance for the detection efficiency. For instance, the process $e^+e^- \rightarrow \gamma\gamma\gamma\gamma$ was first found at VEPP-2M with the ND detector [18] (87 events were observed), while the process of annihilation into five photons can be observed at VEPP-2000.

Interest in such QED processes is due to two reasons:

(1) Advances in experimental techniques give impetus to the development of methods for calculating the cross sections of these processes.

(2) These are background processes in searches for rare hadron reactions—such as $e^+e^- \rightarrow \omega\pi^0 \rightarrow \pi^0\pi^0\gamma \rightarrow 5\gamma$ or $e^+e^- \rightarrow \phi \rightarrow \pi^0e^+e^- \rightarrow e^+e^-\gamma\gamma$; therefore, it is necessary to perform precise calculations for these processes.

5. CONCLUSION

The proposed physics program for VEPP-2000 is quite extensive. Despite a relatively small increase in energy—from 1.4 GeV at VEPP-2M to 2.0 GeV at VEPP-2000—there arise new possibilities in the new energy range that were not available at VEPP-2M:

(1) The uncertainty in measuring the fundamental ratio R will be reduced owing to experiments at VEPP-2000.

(2) It will be possible to perform a thorough investigation of the parameters of the excited vector mesons ρ', ω', and ϕ', their masses lying precisely in the range $2E = 1.4$–2.0 GeV.

(3) Since the VEPP-2000 energy is higher than the τ-lepton mass, $2E > m_\tau$, the CVC hypothesis can be tested throughout the whole range of the τ-lepton-decay spectra.

(4) Since the VEPP-2000 energy is above the threshold for nucleon-pair production, it will be possible to measure the nucleon form factors in the timelike region and to clarify the problem of $N\bar{N}$ bound states.

REFERENCES

1. G. M. Tumaikin, in *Proceedings of the 10th International Conference on High-Energy Particle Accelerators, Serpukhov, 1977,* Vol. 1, p. 443.
2. I. A. Koop *et al.*, Frascati Physics Series **XVI**, 393 (1999).
3. Yu. M. Shatunov *et al.*, in *Proceedings of the 7th European Particle Accelerators Conference EPAC2000, Vienna, Austria, 2000,* p. 439.
4. M. N. Achasov *et al.*, Nucl. Instrum. Methods Phys. Res. A **449**, 125 (2000).
5. M. N. Achasov *et al.*, Nucl. Instrum. Methods Phys. Res. A **441**, 337 (1998); **401**, 179 (1997).
6. V. M. Aulchenko *et al.*, Preprint Budker INP 85-122 (Novosibirsk, 1985).
7. G. N. Abramov *et al.*, Preprint Budker INP 2001-29 (Novosibirsk, 2001).
8. R. R. Akhmetshin *et al.*, Preprint Budker INP 2001-45 (Novosibirsk, 2001).
9. Muon g-2 Collab. (G. W. Benaett *et al.*), hep-ex/0208001.
10. M. Davier *et al.*, Preprint LAL 02-81, Orsay; hep-ex/0208177.
11. R. R. Akhmetshin *et al.*, Phys. Lett. B **527**, 161 (2002).
12. Particle Data Group, Eur. Phys. J. **15** (2000).
13. M. N. Achasov *et al.*, Phys. Lett. B **486**, 29 (2000).
14. A. Antonelli *et al.*, Nucl. Phys. B **517**, 3 (1998).
15. A. B. Clegg and A. Donnache, Z. Phys. C **34**, 257 (1987).
16. V. Benayoun *et al.*, Mod. Phys. Lett. A **14**, 2605 (1999).
17. M. N. Achasov *et al.*, Phys. Lett. B **492**, 8 (2000).
18. S. I. Dolinsky *et al.*, Phys. Rep. **202**, 99 (1991).

Translated by E. Kozlovsky